Paper presented at the 8th International Congress on the Science and Technology of Steelmaking (ICS). Montreal, QC, Canada, Aug. 02-04, 2022 pp. 199-206
The final published version is available at https://doi.org/10.33313/531/021

Post-Mortem Study of Magnesia-Carbon Refractory Bricks Exposed to Thermal Radiation in Electric Arc Furnace Steelmaking

Kianoosh Kaveh[1], Jean-Benoit Morin[2], Mohammad Jahazi[1], Elmira Moosavi-Khoonsari[1]

[1]Department of Mechanical Engineering, École de Technologie Supérieure (ÉTS)
1100 Notre-Dame Street West, Montréal, QC, Canada, H3C 1K3
Phone: +1 (514) 396-8800
Email: Kianoosh.kaveh.1@ens.etsmtl.ca
Mohammad.Jahazi@etsmtl.ca
Elmira.moosavi@etsmtl.ca

[2]Finkl Steel-Sorel
Saint-Joseph-de-Sorel, QC, Canada, J3R 3M8
Phone: +1 (450) 746-4082
Email: Jbmorin@finkl.com

Keywords: Post-Mortem, Magnesia-Carbon Refractory, Scrap-Based Electric Arc Furnace, Steelmaking, Sustainability

INTRODUCTION

The electric arc furnace (EAF) steelmaking route has grown in recent decades, owing to its advantages of treating scraps and direct reduced iron (DRI). The EAF technology and more specifically, the one based on recycling of scraps, largely contributes to reducing the environmental footprint of the steel industry, the preservation of natural resources, and sustainable production. With 0.25-1.15 tons of CO_2 emitted per produced ton of liquid steel (t_{CO2}/t_{LS}), the EAF can be considered superior to the alternative blast furnace-basic oxygen furnace (BF-BOF) route with 1.6-2.2 t_{CO2}/t_{LS} [1, 2]. However, EAF steelmaking faces other industrial challenges which yet remain to be improved/resolved, such as the refractory pre-mature failure and the associated costs which bear on the process through operation downtime, replacement costs for new refractory bricks, and man-hour requirements. Moreover, prolonging the refractory lifetime can largely contribute to waste minimization.

The MgO-C refractory bricks have been widely used as the lining for the EAF because of their superior properties such as high thermal conductivity, low thermal expansion, high temperature mechanical strength, thermal shock resistance, and chemical corrosion resistance. However, the refractory bricks, functioning under extreme operational conditions, may undergo various microstructural changes (*e.g.,* the graphite oxidation, gas phase evolution, formation of phases in the liquid state, and solid-state phase transformations), adversely affecting the thermomechanical properties, and therefore, shortening the refractory lifetime. For instance, the exposure to high thermal radiation from electrodes and the oxidizing atmosphere is detrimental to the service life of the MgO-C bricks [3].

A vast number of lab-scale studies have been conducted in the past few years with the objective to improving the properties of MgO-C refractories. The micro- or nano-carbon/graphite-Si/SiC composites were introduced to the refractory structure to enhance its oxidation resistance [4, 5], or calcium-magnesium-aluminate aggregates were added to improve thermal shock resistance [6]. Cheng et al. [7] studied the effect of carbon content on the mechanical properties of MgO-C refractories. They reported that, although carbon decreased the cold modulus rupture of refractory, it improved the fracture displacement, due to the good sliding ability of the graphite flakes. Liu et al. [8] investigated the effect of carbon content (3-16 wt%) on the oxidation resistance and oxidation kinetics of MgO-C refractories. They revealed that the bulk density, apparent porosity, and cold crushing strength decreased with increasing the carbon content. Xiao et al. [9] also investigated the oxidation behavior of the MgO-C refractories with respect to different Si/SiC contents. The results showed that the deoxidation efficiency of Si is better than that of SiC, and finer grain size and higher surface area of deoxidizers increased the deoxidation efficiency. In addition, the oxidation rate of the refractory at temperatures ranging from 1100°C to 1300°C was mostly dependent on the permeation path of O_2 and contact with C governed by the pore size and distribution in the refractories.

In addition to the small-scale experiments, post-mortem analysis of the MgO-C bricks is essential to better understand the deterioration mechanisms of refractory from both design and operation perspectives, and identify parameters affecting its pre-mature failure in the real context. Calvo et al. [10] studied the degradation mechanism of Al_2O_3-MgO-C (AMC) refractories used in secondary metallurgical ladle furnaces (LF). They reported that an increase in open-pore volume and size, resulting from volatile elimination of the phenolic resin during the first preheating before receiving the molten metal, could be the main cause of refractory degradation. The degradation process would result in increased contact surface between the refractory and liquid steel and molten slag during operation, thereby, accelerating the brick chemical corrosion and erosion by the liquid media. Another similar post-mortem study was carried out by Tabatabaei-Hedeshi et al. [11] on AMC refractories with three

different compositions, used in the LF slag line. The results indicated that the corrosion resistance of the samples containing a stoichiometric spinel ($MgAl_2O_4$) was superior to the ones containing an Al-rich spinel. However, to the best of the authors' knowledge, so far, there is no study reported on the post-mortem bricks from the thermal radiation zone of the EAF. Therefore, the present study aims to investigate the degradation mechanisms of the refractory used in the upper zone of the EAF above the slag line, exposed to thermal radiation, over its service life cycle. The current work will be leveraged to possibly improve the operational parameters and refractory design to prolong the refractory performance in service.

DISCUSSION

1. Sample Acquisition, Preparation, and Characterization

The unprocessed (brand new) and two series of post-mortem MgO-C bricks were acquired from the plant for the investigation. The post-mortem MgO-C refractories were collected from the radiation-, heat-affected zone of the EAF which showed considerable damage.

The bricks were first cut into plates perpendicular to the hot face, as shown in Figure 1. Each plate was sliced into stripes with 1.5cm x 1.8cm cross sections, which were cut down into samples with 2-2.5 cm in length for microstructural investigation. The samples were embedded in the epoxy resin. Two methods of grinding were used, oil and dry grinding. The latter proved to be more convenient for preserving the delicate surface of the post-mortem bricks which had lost their physical integrity to a certain extent. For example, some of the MgO grains detaching from the sample surface during grinding with lapping oil stuck to the SiC paper and disrupted the process. After grinding the samples with 1200 grit SiC paper, they were polished with 1-micron monocrystalline oil-based diamond suspension followed by cleaning with very low water content (<0.05 wt%) isopropanol alcohol in an ultrasonic bath for 15 minutes. Water was avoided during sample preparation to minimize any possible phase alteration in the body of the refractory samples.

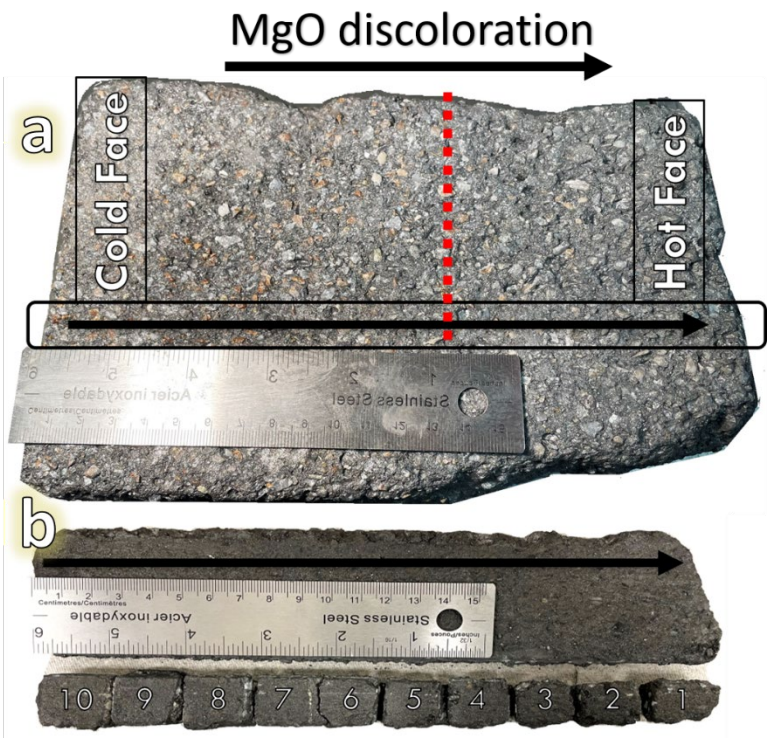

Figure 1. Snapshot of post-mortem MgO-C brick, collected from the radiation, heat-affected zone of EAF; (a) as received and (b) plate cut into smaller samples. The samples were numbered from 1 to 10 from the hot face to the cold face, respectively.

The microstructural and chemical analysis of the unprocessed and post-mortem MgO-C refractory samples was carried out using a Hitachi TM3000 scanning electron microscopy (SEM) coupled with energy dispersive spectroscopy (EDS). The surface of the samples was also observed with the aid of an Olympus LEXT OLS4100 laser confocal microscope.

Illustrative results from samples #1 and #2, the closest to the damaged hot face, are presented in Figure 2. Some results from the analogous unprocessed refractory samples will be also provided for comparison.

2. Equilibrium Thermodynamic Simulation

The thermochemical evolutions of the MgO-C brick were simulated over a wide temperature range using the thermodynamic software FactSage™ version 8.1 [12].Thermodynamic descriptions of the pure components and the gas phase were taken from the FactPS database, and thermodynamic properties of oxide components were adopted from the FToxid database. In combination with the microstructural analysis of post-mortem bricks, thermodynamic modeling can contribute to a better understanding of the chemical reactions and phase transformations, underlying the refractory degradation during the service.

3. Results

3.1. Optical Microscopy

Figure 2 illustrates the optical microscopy image of a sintered coarse MgO grain, consisting of a number of finer MgO grains, from the post-mortem sample #1 (see Figure 1). There is a clear discoloration from the rim in contact with the graphite matrix to the core of the grain (*i.e.*, the core appears in orange and the rim appears in light grey). In addition, the discoloration of orangish MgO grains from the hot face to the cold face can be observed in Figure 1. This could be attributed to an alteration in chemical composition of the MgO grains, *e.g.*, the change in the oxidation state of iron oxide from hematite (Fe^{3+}) to wüstite (Fe^{2+}) or metallic iron (Fe).

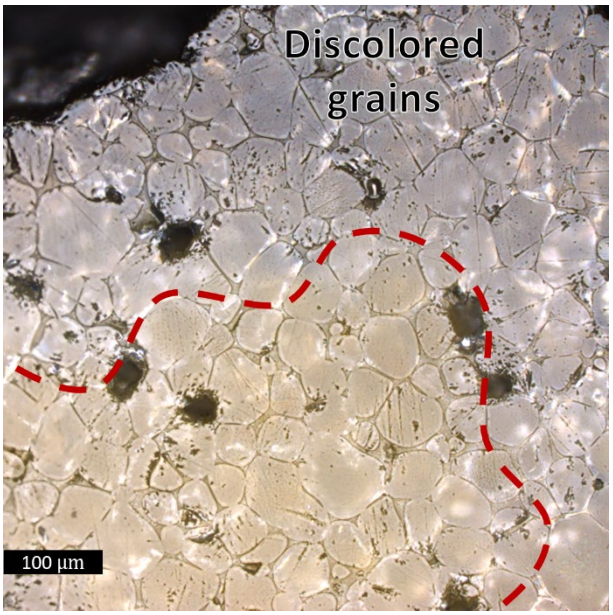

Figure 2. Optical microscopy image from a sintered coarse MgO grain, undergoing discoloration from the rim to the center. The red line shows an approximate border between the discolored and original regions.

2.2. SEM-EDS Analysis

Back-scattered electron (BSE) image and elemental maps of an unprocessed MgO-C sample are presented in Figure 3. As seen, the MgO particles with a wide range of size distribution are embedded in the graphite matrix. A glass phase was also found inside the MgO grains, which is considered to be impurity. The quality of the MgO grains in terms of impurities and discontinuities is different, which can be hardly observed at this magnification. In addition, particles of Al and/or Si are observed in the figure, which are incorporated into the brick microstructure to act as deoxidizers. The deoxidizers are expected to react with and consume oxygen to protect graphite from oxidation. Figure 4 shows that based on the selective oxidation mechanism, Al and Si react with oxygen prior to graphite (or carbon) to prevent C oxidation and formation of CO(g), which should be minimized to avoid the porosity formation. The development of porosity and enlargement of the existing porosities deteriorate the refractory integration. As shown in Figure 4, Si loses its deoxidation ability above 1650 °C.

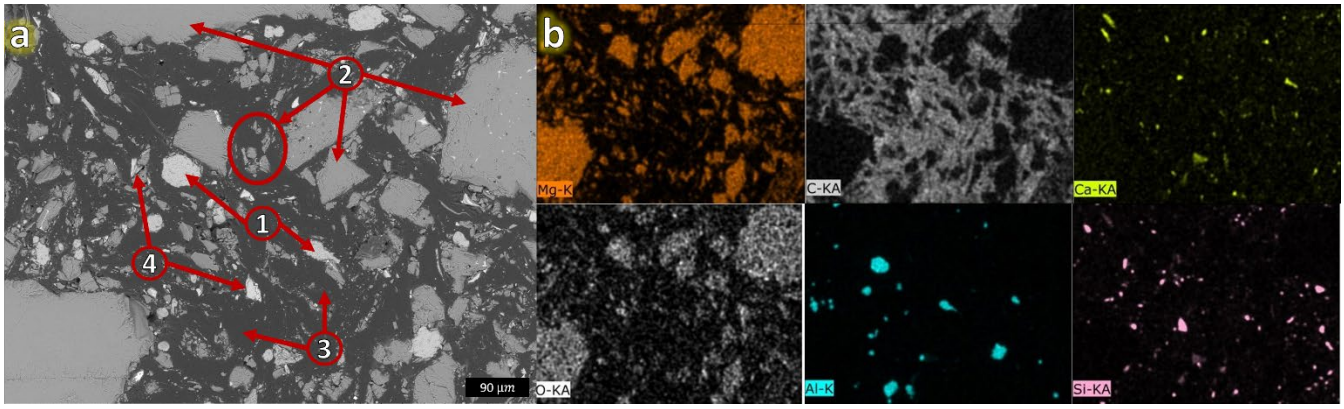

Figure 3. Unprocessed refractory; (a) BSE image and (b) EDS elemental maps. (1) Al deoxidizer particles, (2) MgO grains, (3) graphite matrix, and (4) Si deoxidizer particles.

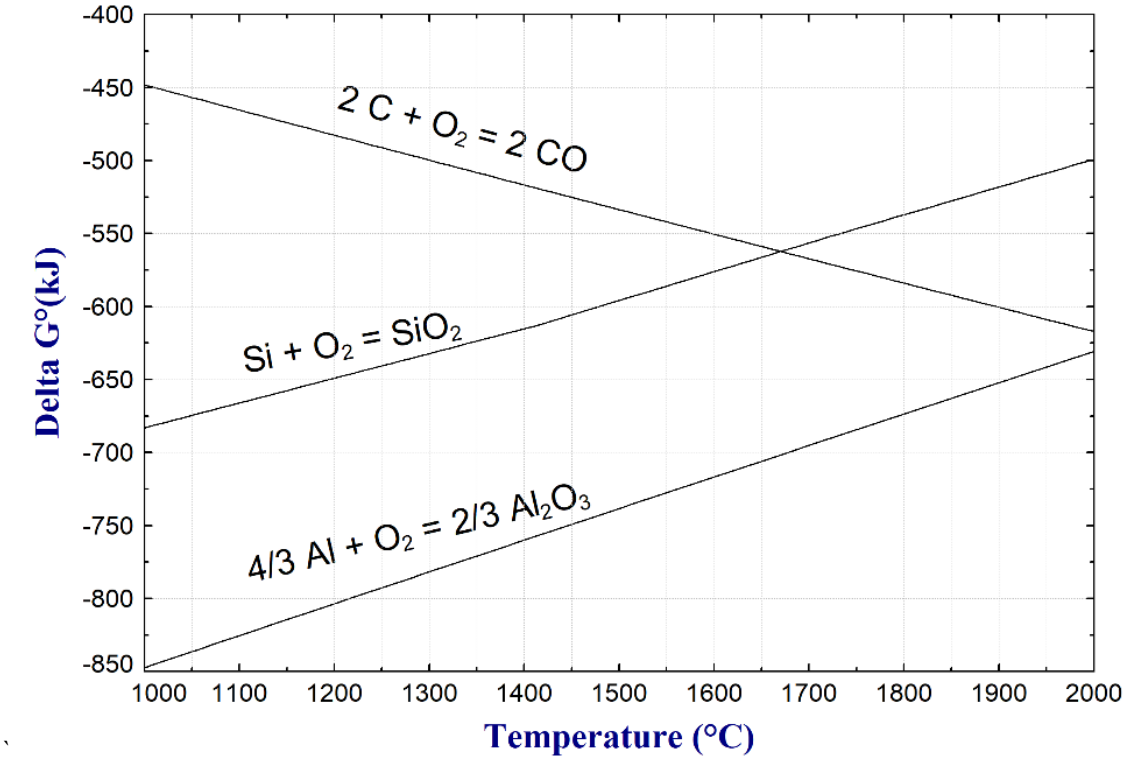

Figure 4. Standard Gibbs energy of formation of oxides of Al and Si from their constituent metal and 1 mole of oxygen gas in comparison to C oxidation, calculated using FactSage 8.1 [12].

Figure 5 depicts the BSE image of the post-mortem refractory, sample #1 (see Figure 1). It is seen that refractory microstructure underwent some severe changes during service, and the brick has lost its overall integrity. The Al deoxidizer grains appear to have fully oxidized to form alumina, and the adjacent graphite flakes are fibrous, leaving behind a porous matrix. For example, the development of porosity in the microstructure can enhance the gas infiltration from the surface into the body of the refractory and subsequent gas/liquid/solid reactions The grains of Si deoxidizer could not be located in the post-mortem samples. Iron particles seen in figure 5 probably stemmed from an external source such as charged scraps into the EAF.

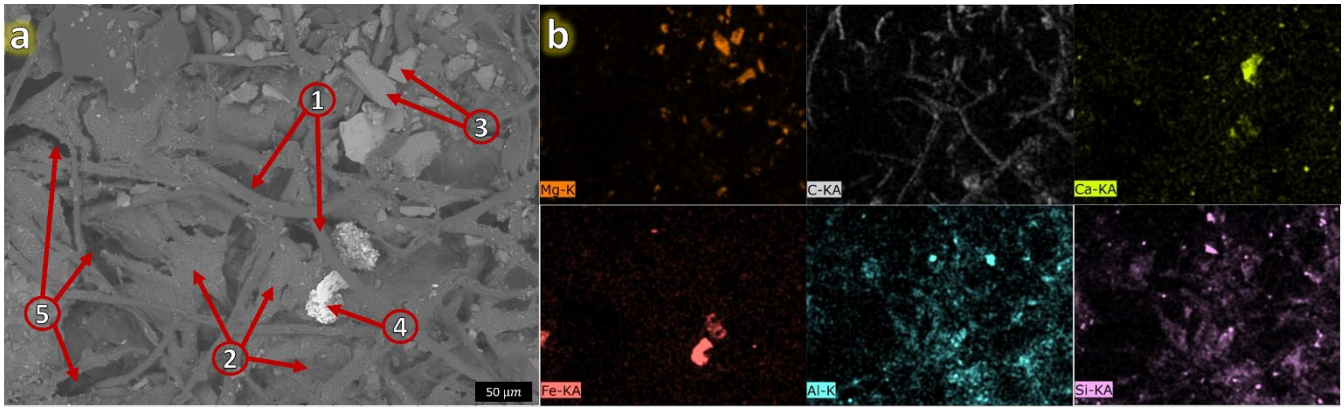

Figure 5. Post-mortem refractory taken from hot face (sample #1); (a) BSE image and (b) EDS elemental maps. (1) fibrous graphite structure, (2) aluminosilicate grains formed from oxidation of deoxidizers, (3) MgO particles, (4) Fe particle, and (5) porosity.

2.3 Thermodynamic Simulation

Thermodynamic simulation of the refractory self-reaction was conducted based on its nominal bulk composition, listed in Table 1. In addition to graphite and MgO, which are the main constituents of the refractory, the MgO grains can contain up to 2 wt% glass (CaO-SiO_2-Al_2O_3-Fe_2O_3) as impurity. Self-reaction means chemical reactions between the refractory constituents themselves exposed to high temperatures, without being in contact with an external body such as slag, steel, and/or oxidizing/reducing gas.

Table 1. MgO-C refractory nominal composition (in wt.%)

MgO	SiO_2	CaO	Al_2O_3	Fe_2O_3	Residual C
80.36	0.32	0.62	0.29	0.25	18-20

Figure 6 illustrates the calculated phase evolutions versus temperature within the body of the MgO-C refractory. The interior and exterior frames show the stable phases for 100% and 2% total mass, respectively. According to the calculations, MgO and C are stable over a wide temperature range. However, at high temperatures, above 1750 °C, the amount of gas phase steeply increases at the expense of MgO and C, leading to the formation of CO(g) and Mg(v) gaseous components. In addition to the major phases, other phases in minor quantities are calculated to be stable at high temperatures such as liquid slag, Fe_3C, and the calcium-alumina-silicate phase (present in two different polymorphs of β- and α-C_2SA). At about 1450 °C, the liquid slag starts forming, and its major constituents are CaO, SiO_2, MgO, and Al_2O_3. The gas evolution and liquid slag formation in the body of the refractory can severely deteriorate its internal integration. In addition, any phase change/transformation can be harmful to the thermomechanical resistance of the refractory. The refractory self-reactions, under the influence of the existing thermal gradient across the body of refractory lining, may play an important role in the determination of the brick lifetime. Such analysis has been used to explain some of the mechanisms underlying the submerged entry nozzle degradation in the steel continuous casting [13, 14].

Other phases which were calculated to be stable over a wide range of temperature below 1200 °C are $Ca_7Mg(SiO_4)_4$ (bredigite), $Ca_5(SiO_4)_2CO_3$, $Ca_3MgAl_4O_{10}$, and $MgAl_2O_4$ (spinel). The gas generation at temperatures as low as 750 °C is attributed to the decomposition of the carbonate phase calculated to be originally stable. To validate the presence of low temperature phases in the body of the refractory, post-mortem samples (# 5-10) from the refractory cold face should be microstructurally characterized. However, the study of the unprocessed bricks has not revealed the presence of these phases yet. It might be that these phases occur in very small concentrations that cannot be easily located under microscope. Besides, it should be noted that the simulation considered global equilibrium state between the brick constituents. However, in reality, the equilibrium state might not be achieved because of the slow kinetics of chemical reactions in the solid state. In addition, there might be only several local equilibria in the body of the refractory, instead of a global equilibrium.

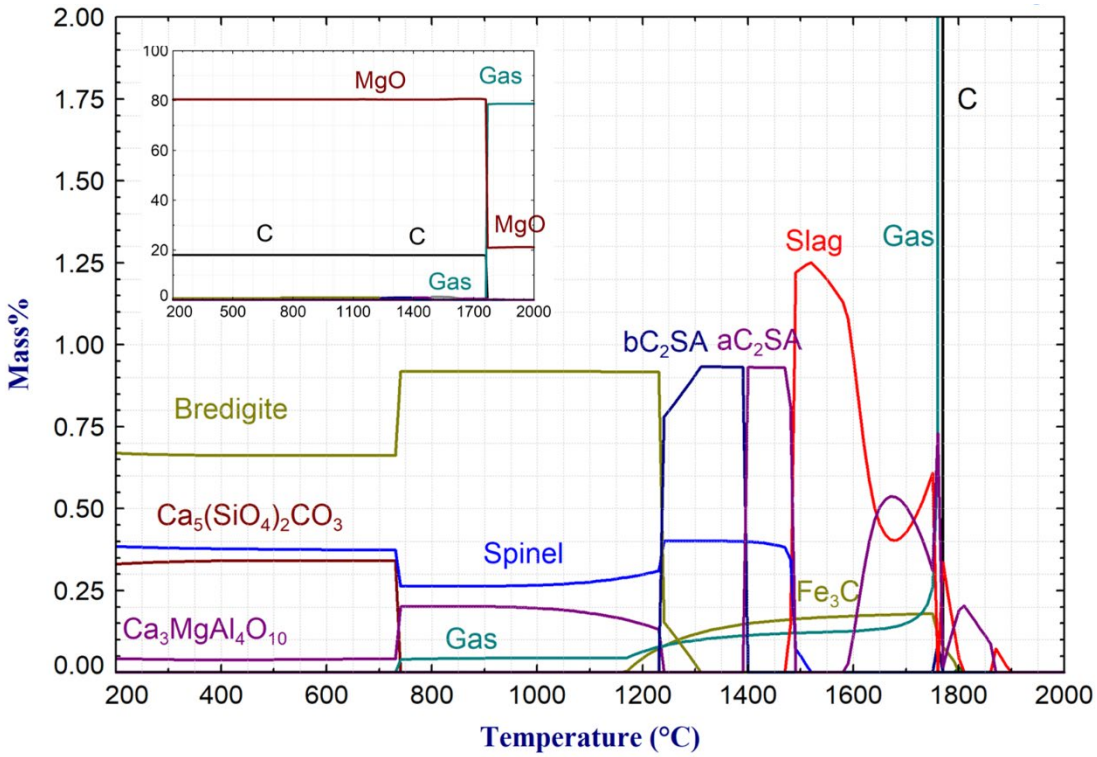

Figure 6. Self-reaction of the MgO-C refractory versus temperature, showing stable phases for 2% of total mass, calculated using FactSage 8.1 [12]. The interior frame shows the stable phases for 100% of total mass. Bredigite: $Ca_7Mg(SiO_4)_4$; Spinel: $MgAl_2O_4$; C_2SA: $Ca_2SiAl_2O_7$.

CONCLUSIONS

The purpose of this study was to investigate the degradation mechanisms of the MgO-C bricks used as EAF upper zone lining above the slag line, exposed to thermal radiation from electrodes. Therefore, the hot face of post-mortem bricks from the plant was studied and compared to unprocessed ones. Moreover, thermodynamic simulation of the refractory self-reaction was performed for better comprehension of the thermophysical phenomena underlying the refractory degradation. Some of the most important findings, are summarized below.

The most significant features of unprocessed refractory were MgO grains with a wide size distribution, calcium-silicate glass as impurity within the MgO grains, deoxidizers such as Al and Si, graphite matrix as the binder, and original porosities.

The post-mortem bricks underwent sever microstructural alteration such as graphite flakes fibrosis, new porosity formation, MgO grain discoloration due to phase transformation, and oxidation of Al grains. These microstructural evolutions can be alone detrimental to the brick performance and/or accelerate other physicochemical phenomena weakening the refractory integrity.

Equilibrium thermodynamic calculations revealed the possibility of brick self-reactions at high temperatures such as the CO(g) and Mg(v) evolution and liquid slag formation. The former leads to new porosity development in the body of the refractory, and the latter explains the detrimental effect of impurity on the integrity of the bricks. Moreover, from the process perspectives, improvement to the operation practice such as better protection of the bricks' hot face from the high thermal radiation might be efficient in preventing the refractory pre-mature failure.

ACKNOWLEDGEMENT

The authors would like to acknowledge Finkl Steel-Sorel and Mitacs Accelerate Program (IT28458) for financial support of the project. In addition, the authors highly appreciate Finkl Steel-Sorel for providing the MgO-C refractory bricks.

REFERENCES

1. Kirschen, M., T. Hay, and T. Echterhof, *Process Improvements for Direct Reduced Iron Melting in the Electric Arc Furnace with Emphasis on Slag Operation.* Processes, 2021. **9**(2): p. 402.
2. Pardo, N. and J.A. Moya, *Prospective scenarios on energy efficiency and CO2 emissions in the European Iron & Steel industry.* Energy, 2013. **54**: p. 113-128.
3. Volkova, O., P.R. Scheller, and B. Lychatz, *Kinetics and thermodynamics of carbon isothermal and non-isothermal oxidation in MgO-C refractory with different air flow.* Metallurgical and Materials Transactions B, 2014. **45**(5): p. 1782-1792.
4. Raju, M., et al., *Improvement in the properties of low carbon MgO-C refractories through the addition of graphite-SiC micro-composite.* Journal of the European Ceramic Society, 2022. **42**(4): p. 1804-1814.
5. Li, Y., et al., *Catalytic preparation of carbon nanotube/SiC whisker bonded low carbon MgO–C refractories and their high-temperature mechanical properties.* Ceramics International, 2022. **48**(4): p. 5546-5556.
6. Chen, Q., et al., *Improved thermal shock resistance of MgO–C refractories with addition of calcium magnesium aluminate (CMA) aggregates.* Ceramics International, 2022. **48**(2): p. 2500-2509.
7. Cheng, Y., et al., *Microstructure and properties of MgO–C refractory with different carbon contents.* Ceramics International, 2021. **47**(2): p. 2538-2546.
8. Liu, Z., et al., *Effect of carbon content on the oxidation resistance and kinetics of MgO-C refractory with the addition of Al powder.* Ceramics International, 2020. **46**(3): p. 3091-3098.
9. Xiao, J., et al., *Oxidation behaviors of MgO-C refractories with different Si/SiC ratio in the 1100–1500 C range.* Ceramics international, 2019. **45**(17): p. 21099-21107.
10. Calvo, W.A., P. Pena, and A.G.T. Martinez, *Post-mortem analysis of alumina-magnesia-carbon refractory bricks used in steelmaking ladles.* Ceramics International, 2019. **45**(1): p. 185-196.
11. Tabatabaie-Hedeshi, S., M. Bavand-vandchali, and R. Naghizadeh, *Characterization and post-mortem analysis of Al2O3-MgO-C refractories used in steelmaking ladle furnaces.* Engineering Failure Analysis, 2020. **116**: p. 104697.
12. Bale, C.W., et al., *FactSage thermochemical software and databases.* Calphad, 2002. **26**(2): p. 189-228.
13. Zinngrebe, E., et al., *Microstructures of mould slag crawling at the SEN during thin slab casting.* 2019.
14. Moosavi-Khoonsari, E., et al., *Thermodynamic modeling of refractory/mould slag/steel interactions concerning slag crawling.* 2019.